

Charged Dilatonic Black Holes in Gravity's Rainbow

S. H. Hendi^{1,2*}, Mir Faizal^{3†}, B. Eslam Panah^{1 ‡} and S. Panahiyan^{1,4 §}

¹*Physics Department and Biruni Observatory, College of Sciences, Shiraz University, Shiraz 71454, Iran*

²*Research Institute for Astronomy and Astrophysics of Maragha (RIAAM), Maragha, Iran*

³*Department of Physics and Astronomy, University of Waterloo, Waterloo, Ontario, N2L 3G1, Canada*

⁴*Physics Department, Shahid Beheshti University, Tehran 19839, Iran*

In this paper, we present charged dilatonic black holes in gravity's rainbow. We study geometric and thermodynamic properties of black hole solutions. We also investigate the effects of rainbow functions on different thermodynamic quantities for these charged black holes in dilatonic gravity's rainbow. Then, we demonstrate that first law of thermodynamics is valid for these solutions. After that, we investigate thermal stability of the solutions using canonical ensemble and analyze the effects of different rainbow functions on thermal stability. In addition, we present some arguments regarding the bound and phase transition points in context of geometrical thermodynamics. We also study the phase transition in extended phase space in which cosmological constant is treated as the thermodynamic pressure. Finally, we use another approach to calculate and demonstrate that obtained critical points in extended phase space are representing a second order phase transition for these black holes.

I. INTRODUCTION

Motivated by works on Lifshitz scaling in condensed matter physics, it is possible to take different Lifshitz scaling for space and time, and the resultant theory is called Horava-Lifshitz gravity [1, 2]. In the IR limit this gravity reduces to general relativity, and so it can be considered as a UV completion of general relativity. Motivated by this work on Horava-Lifshitz gravity, different Lifshitz scaling for space and time have been considered for type IIA string theory [3], type IIB string theory [4], AdS/CFT correspondence [5–8], dilatonic black branes [9, 10], and dilatonic black holes [11, 12]. Another UV completion theory of general relativity which reduces to general relativity in the IR limit is called gravity's rainbow [13]. In fact, it has been demonstrated that gravity's rainbow is related to Horava-Lifshitz gravity [14]. This is because both of these theories are based on the modifying the usual energy-momentum dispersion relation in the UV limit such that it reduces to the usual energy-momentum dispersion relation in the IR limit. It may be noted that such modification of the usual energy-momentum has also been obtained in discrete spacetime [15], spacetime foam [16], spin-network in loop quantum gravity (LQG) [17], ghost condensation [18] and non-commutative geometry [19, 20]. The non-commutative geometry occurs due to background fluxes in string theory [21, 22], and is used to derive one of the most important rainbow functions in gravity's rainbow [23, 24].

It may be noted that the UV modification of the usual energy-momentum relation implies the breaking of the Lorentz symmetry in the UV limit of the theory. The spontaneous breaking of the Lorentz symmetry can occur in string theory because of the existence of an unstable perturbative string vacuum [25]. It is possible for a tachyon field to have wrong sign for its mass squared in string field theory, and this causes the perturbative string vacuum to become unstable. The theory becomes ill-defined if the vacuum expectation value of the tachyon field is infinite. It is also possible for the vacuum expectation value of the tachyon field to be finite and negative. In this case, the coefficient of the quadratic term for the massless vector field is nonzero and negative, and this breaks the Lorentz symmetry. The spontaneous breaking of the Lorentz symmetry in string theory has also been investigated using the gravitational version of the Higgs mechanism [26]. This has been done for the low energy effective action obtained from string theory. The Lorentz symmetry breaking has been also studied using black brane in type IIB string theory [27]. In this analysis, moduli stabilization was studied using a KKLT-type moduli potential in the context of type IIB warped flux compactification. It was demonstrated that a Higgs phase for gravity will exist if all moduli are stabilized. Another study regarding the breaking of Lorentz symmetry was done by using compactification in string field theory [28]. It may be noted that various other approaches to quantum gravity also indicate that the Lorentz symmetry might only be an effective symmetry which occurs in the IR limit of some fundamental theories of quantum gravity [29–33].

Hence, there is a good motivation to study the UV deformation of geometries that occur in string theory. In fact,

* email address: hendi@shirazu.ac.ir

† email address: f2mir@uwaterloo.ca

‡ email address: behzad.eslampanah@gmail.com

§ email address: sh.panahiyan@gmail.com

motivated by Lifshitz deformation of such geometries, and the relation between Horava-Lifshitz gravity and gravity's rainbow [14], recently rainbow deformation of geometries that occur in string theory has been performed. Thus, the modifications of the thermodynamics of black rings has been analyzed using gravity's rainbow [34]. It has been observed that a remnant exists for black rings in gravity's rainbow. It has also been argued that a remnant might exist for all black objects in gravity's rainbow [35]. This has been explicitly demonstrated for Kerr black holes, Kerr-Newman black holes in de Sitter space, charged AdS black holes, higher dimensional Kerr-AdS black holes and black saturn [35]. This was done by generalizing the work done on the thermodynamics of black holes in gravity's rainbow [36]. As the usual uncertainty principle still holds in gravity's rainbow [37, 38], and it is possible to obtain a lower bound on the energy $E \geq 1/\Delta x$, using the usual uncertainty principle. This energy can be related to the energy of a particle emitted in Hawking radiation. Furthermore, the value of the uncertainty in position can be equated to the radius of the event horizon, $E \geq 1/\Delta x \approx 1/r_+$. This energy can be related to the energy at which spacetime is probed, and hence it describes the energy E in gravity's rainbow. This is because effectively this particle emitted with the energy E can be viewed as a probe which is probing the geometry of the black hole. This consideration modifies the temperature of the black hole [36]. The entropy and heat capacity of black hole in gravity's rainbow can be calculated using this modified temperature. An interesting consequence of this modified solution is that it predicts the existence of remnants for the black hole. Thus, the temperature of the black hole reduces to zero, when black hole has a small but finite size. At this size, the black hole does not emit any Hawking radiation. The existence of black hole remnants can be used as a solution for the information paradox [39, 40]. Furthermore, it also solves problem related to the existence of naked singularity at the last stage of the evaporation of a black hole. As in this picture, a black hole does not evaporate completely producing a naked singularity, but rather a remnant is produced at the last stage of the evaporation of the black hole. The existence of a remnant also has phenomenological consequences. This is because it is not possible to produce black holes smaller than these remnants. This increases the energy at which mini black holes can be produced at the LHC [41]. Recently, a lot of interest has been generated in gravity's rainbow [42–47]. It may be noted that the rainbow functions have been constrained from experimental data [47]. Black hole solutions in gravity's rainbow with nonlinear sources have been investigated in [48]. In addition, the hydrostatic equilibrium equation for this gravity was obtained in Ref. [49].

As there is a strong motivation to study rainbow deformation of geometries that occur in string theory, so we analyze the rainbow deformation of charged dilatonic black holes in this paper. It may be noted that dilaton gravity arises as a low-energy effective field theory of string theory [50, 51]. The dilaton field is also a candidate for dark matter [52]. In fact, in order to have better picture of nature of the dark energy, a new scalar field is added to the field content of the original theory [53, 54]. Black objects in presence of dilaton gravity, have also been investigated [55–57]. Recently, dilaton field has been used for analyzing compact objects and hydrostatic equilibrium of stars [58, 59]. The evaporation of quantum black holes has also been investigated using two dimensional dilaton gravity [60, 61]. Motivated by these applications, we analyze dilaton field using the formalism of gravity's rainbow.

Thermodynamical aspects of black holes have been of a great interest ever since of pioneering works of Hawking and Beckenstein [62, 63]. The idea that geometrical aspects of black holes could be interpreted as thermodynamical quantities provides a deep insight into the connection between gravity and quantum mechanics. On the other hand, introduction and developments in gauge/gravity duality highlighted the importance of black holes thermodynamics [64–78]. In addition, Hawking and Page showed the existence of a phase transition for asymptotically anti de-Sitter black holes [79]. This phase transition was reconsidered through the use of AdS/CFT correspondence by Witten [80]. These works motivated a large number of researches to be conducted in context of black holes thermodynamics, stability and their phase transitions [81–90].

Recently, it has been demonstrated that, it is possible to treat the cosmological constant as the thermodynamic pressure in extended phase space. There are several reasons for such consideration which among them one can point out the existence of second order phase transition for black holes, Van der Waals like liquid/gas behavior in phase diagrams and formation of the triple point [91–109]. The consideration of the cosmological constant as a thermodynamical variable could be supported by studies that are conducted in context of AdS/CFT [120–123]. In addition, it was shown that a case of ensemble dependency exists for charged 3-dimensional black holes which could be removed by considering cosmological constant as a thermodynamical variable [124]. The thermodynamical critical behavior of black holes in presence of different matter fields and gravities has been investigated in literature [91–109]

Another interesting method of studying thermodynamical structure of the black holes is through the use of geometry. It is proposed that one can build a phase space of the black holes by employing one of thermodynamical quantities of the black holes as thermodynamical potential and its corresponding extensive parameters as components of the phase space. The information regarding phase transitions of the black holes is within the singularities of Ricci scalar of the constructed phase space. In other words, the divergencies of the Ricci scalar of thermodynamical metric are representing bound and phase transition points. The thermodynamical potential for this method could be mass which is used in Weinhold [110, 111], Quevedo [112–114] and HPEM [115–117] metrics or entropy which is employed in Ruppeiner [118, 119] metric. It was pointed out that Ruppeiner and Weinhold methods are related to each other with

temperature as conformal factor [112–114]. It was shown that for specific cases of black holes, Weinhold, Ruppeiner and Quevedo metrics may fail to provide consistent results regarding phase transitions while the HPEM metric is proven to be successful one [115–117]. In what follows, we use all of these methods to study phase transitions of the black holes.

This paper is organized as follows. We obtain the charged black hole solutions in dilaton gravity's rainbow and analyze their properties. This will be done by making the metric of charged black hole solutions in dilaton gravity depends on the energy. We also examine the first law of thermodynamics for this solution. Next, we study the stability of such solutions in gravity's rainbow and phase transition of these black holes through heat capacity, geometrical thermodynamics and the analogy between cosmological constant and thermodynamical pressure. Finally, we obtain critical pressure and horizon radius through another method. Last section is devoted to conclusion.

II. CHARGED DILATONIC BLACK HOLE SOLUTIONS IN GRAVITY'S RAINBOW

In this section, we obtain charged black hole solutions in dilaton gravity's rainbow and investigate their properties. This will be done by writing an energy dependent version of the metric for dilaton-Maxwell gravity. It may be noted that gravity's rainbow is based on the generalization of doubly special relativity [125], and so it is not possible for a particle to attain energy greater than the Planck energy in gravity's rainbow. This is because gravity affects particles of different energies differently, and so the spacetime is represented by a family of energy dependent metrics in gravity's rainbow [13]. The gravity's rainbow can be constructed by considering the following deformation of the standard energy-momentum relation

$$E^2 f^2(\varepsilon) - p^2 g^2(\varepsilon) = m^2, \quad (1)$$

where energy ratio is $\varepsilon = E/E_P$, in which E and E_P are, respectively, the energy of test particle and the Planck energy. The functions $f(\varepsilon)$ and $g(\varepsilon)$ are required to be constrained in such a way that the standard energy-momentum relation is obtained in the infrared limit. Thus, we require

$$\lim_{\varepsilon \rightarrow 0} f(\varepsilon) = 1, \quad \lim_{\varepsilon \rightarrow 0} g(\varepsilon) = 1. \quad (2)$$

It may be noted that the spacetime is probed at the energy E , and by definition this cannot be greater than the Planck energy. $f^2(\varepsilon)$ and $g^2(\varepsilon)$ are called the rainbow functions and their functional forms are phenomenologically motivated. Now it is possible to define an energy dependent deformation of the metric $\hat{g}(\varepsilon)$ as [126]

$$\hat{g}(\varepsilon) = \eta^{ab} e_a(\varepsilon) \otimes e_b(\varepsilon), \quad (3)$$

where

$$e_0(\varepsilon) = \frac{1}{f(\varepsilon)} \tilde{e}_0, \quad e_i(\varepsilon) = \frac{1}{g(\varepsilon)} \tilde{e}_i, \quad (4)$$

here \tilde{e}_0 and \tilde{e}_i refer to the energy independent frame fields.

The 4-dimensional action of charged dilaton gravity is [127]

$$\mathcal{I} = \frac{1}{16\pi} \int d^4x \sqrt{-g} \left[\mathcal{R} - 2(\nabla\Phi)^2 - V(\Phi) - e^{-2\alpha\Phi} F_{\mu\nu} F^{\mu\nu} \right], \quad (5)$$

where \mathcal{R} is the Ricci scalar curvature, Φ is the dilaton field and $V(\Phi)$ is a potential for Φ . The electromagnetic field is $F_{\mu\nu} = \partial_\mu A_\nu - \partial_\nu A_\mu$ in which A_μ is the electromagnetic potential. In addition, it should be pointed out that α is a constant which determines the strength of coupling of the scalar and electromagnetic field. Due to the fact that we are looking for the black hole with a radial electric field ($F_{tr}(r) = -F_{rt}(r) \neq 0$), the electromagnetic potential will be in the following form

$$A_\mu = \delta_\mu^0 h(r). \quad (6)$$

Using variational principle and varying Eq. (5) with respect to the gravitational field $g_{\mu\nu}$, the dilaton field Φ and the gauge field A_μ , we can obtain the following field equations

$$R_{\mu\nu} = 2 \left(\partial_\mu \Phi \partial_\nu \Phi + \frac{1}{4} g_{\mu\nu} V(\Phi) \right) + 2e^{-2\alpha\Phi} \left(F_{\mu\eta} F_\nu^\eta - \frac{1}{4} g_{\mu\nu} F_{\lambda\eta} F^{\lambda\eta} \right), \quad (7)$$

$$\nabla^2 \Phi = \frac{1}{4} \frac{\partial V}{\partial \Phi} - \frac{\alpha}{2} e^{-2\alpha\Phi} F_{\lambda\eta} F^{\lambda\eta}, \quad (8)$$

$$\nabla_\mu (e^{-2\alpha\Phi} F^{\mu\nu}) = 0. \quad (9)$$

In this paper we are attempting to obtain dilaton-Maxwell rainbow solutions. To do so, one can employ following static metric ansatz

$$ds^2 = -\frac{\Psi(r)}{f^2(\varepsilon)} dt^2 + \frac{1}{g^2(\varepsilon)} \left[\frac{dr^2}{\Psi(r)} + r^2 R^2(r) d\Omega_k^2 \right], \quad (10)$$

where $\Psi(r)$ and $R(r)$ are radial dependent functions which should be determined, and $d\Omega_k^2$ represents the line element of a 2– dimensional hypersurface with the constant curvature $2k$ and volume ϖ_2 . We should note that the constant k indicates that the boundary of $t = \text{constant}$ and $r = \text{constant}$ can be a positive (elliptic), zero (flat) or negative (hyperbolic), constant curvature hypersurface with following explicit forms

$$d\Omega_k^2 = \begin{cases} d\theta^2 + \sin^2 \theta d\varphi^2, & k = 1 \\ d\theta^2 + \sinh^2 \theta d\varphi^2, & k = -1 \\ d\theta^2 + d\varphi^2, & k = 0 \end{cases}. \quad (11)$$

Using Eq. (9), one can obtain electromagnetic tensor as

$$F_{tr} = \frac{qe^{2\alpha\Phi}}{r^2 R(r)^2}, \quad (12)$$

where q is an integration constant which is related to the electric charge of the black hole.

Here, in order to find consistent metric functions, we use a modified version of Liouville-type dilation potential with following form

$$V(\Phi) = \frac{2k\alpha^2}{b^2 \mathcal{K}_{-1,1}} g^2(\varepsilon) e^{\frac{2\Phi}{\alpha}} + 2\Lambda e^{2\alpha\Phi}, \quad (13)$$

where $\mathcal{K}_{i,j} = i + j\alpha^2$ and Λ is a free parameter which plays the role of the cosmological constant. It is worthwhile to mention that for the case of $g(\varepsilon) = f(\varepsilon) = 1$, one obtains

$$\lim_{g(\varepsilon)=f(\varepsilon)\rightarrow 1} V(\Phi) = \frac{2k\alpha^2}{b^2 \mathcal{K}_{-1,1}} e^{\frac{2\Phi}{\alpha}} + 2\Lambda e^{2\alpha\Phi}, \quad (14)$$

which is the usual Liouville-type dilation potential that is used in the context of Friedman-Robertson-Walker scalar field cosmologies [128] and Einstein-Maxwell-dilaton black holes [127, 129, 130].

Next, we employ an ansatz, $R(r) = e^{\alpha\Phi(r)}$, in the field equations. The motivation for considering such an ansatz is due to black string solutions of Einstein-Maxwell-dilaton gravity which was first introduced in Ref. [131]. Now, we are in a position to obtain metric functions. It is a matter of calculation to show that by using Eq. (12), the metric (10) and the mentioned ansatz for $R(r)$, we have following solutions for the field equations, (Eqs. (7) and (8))

$$\Psi(r) = -\frac{\mathcal{K}_{1,1}}{\mathcal{K}_{-1,1}} \left(\frac{b}{r}\right)^{-2\gamma} k - \frac{m}{r^{\frac{\mathcal{K}_{1,-1}}{\mathcal{K}_{1,1}}}} + \frac{\mathcal{K}_{1,1}^2 \Lambda r^2}{g^2(\varepsilon) \mathcal{K}_{-3,1}} \left(\frac{b}{r}\right)^{2\gamma} + \frac{q^2 \mathcal{K}_{1,1} f^2(\varepsilon)}{r^2} \left(\frac{b}{r}\right)^{-2\gamma}, \quad (15)$$

$$\Phi(r) = \frac{\alpha}{\mathcal{K}_{1,1}} \ln \left(\frac{b}{r}\right), \quad (16)$$

where b is an arbitrary constant and $\gamma = \alpha^2/\mathcal{K}_{1,1}$. In the above expression, m is an integration constant which is related to the total mass of the black hole. It is notable that, in the absence of a non-trivial dilaton ($\alpha = \gamma = 0$), the solution (15) reduces to

$$\Psi(r) = k - \frac{m}{r} - \frac{\Lambda}{3} \frac{r^2}{g^2(\varepsilon)} + \frac{f^2(\varepsilon) q^2}{r^2}, \quad (17)$$

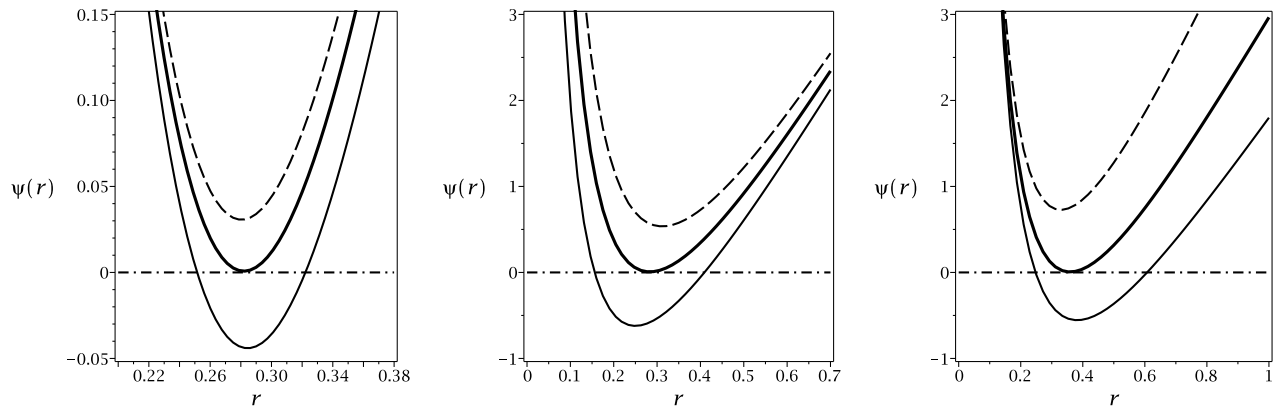


FIG. 1: $\Psi(r)$ versus r for $k = 1$, $m = 5$, $\Lambda = -0.5$, $b = 1.2$ and $q = 0.68$.

Left panel for $\alpha = 0.9$, $f^2(\varepsilon) = 1$, $g^2(\varepsilon) = 0.85$ (dashed line), $g^2(\varepsilon) = 0.96$ (bold line) and $g^2(\varepsilon) = 1.20$ (continuous line). Middle panel for $\alpha = 0.9$, $g^2(\varepsilon) = 1$, $f^2(\varepsilon) = 0.80$ (dashed line), $f^2(\varepsilon) = 1.05$ (bold line) and $f^2(\varepsilon) = 1.20$ (continuous line). Right panel for $g^2(\varepsilon) = 1.3$, $f^2(\varepsilon) = 1.3$, $\alpha = 0.85$ (dashed line), $\alpha = 0.87$ (bold line) and $\alpha = 0.9$ (continuous line).

which describes a 4-dimensional asymptotically AdS topological charged black hole in gravity's rainbow with a positive, zero or negative constant curvature hypersurface.

In order to confirm black hole interpretation of the solutions, we look for the curvature singularity. To do so, we calculate the Kretschmann scalar. Calculations show that for finite values of radial coordinate, the Kretschmann scalar is finite. On the other hand, for very small and very large values of r , we obtain

$$\lim_{r \rightarrow 0} R_{\alpha\beta\mu\nu} R^{\alpha\beta\mu\nu} \propto r^{-\frac{4\mathcal{K}_{2,1}}{\mathcal{K}_{1,1}}}, \quad (18)$$

$$\lim_{r \rightarrow \infty} R_{\alpha\beta\mu\nu} R^{\alpha\beta\mu\nu} = \frac{12\Lambda(\alpha^4 - 2\alpha^2 + 2)}{\mathcal{K}_{3,-1}^2} \left(\frac{b}{r}\right)^{4\gamma}. \quad (19)$$

Equation (18) confirms that there is an essential singularity located at $r = 0$, while Eq. (19) shows that for nonzero α , the asymptotical behavior of the solutions is not AdS. It is easy to show that the metric function may contain real positive roots (see Fig. 1), and therefore, the curvature singularity can be covered with an event horizon and interpreted as a black hole.

III. THERMODYNAMICAL QUANTITIES

Now, we are in a position to calculate thermodynamic and conserved quantities of obtained solutions and examine the validity of the first law of thermodynamics.

In order to obtain the temperature, we use the concept of surface gravity to show that the temperature of these solutions has following form

$$T = -\frac{g(\varepsilon)\mathcal{K}_{1,1}\left(\frac{b}{r_+}\right)^{-2\gamma}}{4\pi} \left[\frac{q^2 f(\varepsilon)}{r_+^3} + \frac{r_+ \Lambda}{g^2(\varepsilon) f(\varepsilon)} \left(\frac{b}{r_+}\right)^{4\gamma} + \frac{k}{f(\varepsilon) r_+ \mathcal{K}_{-1,1}} \right]. \quad (20)$$

On the other hand, one can use the area law for extracting modified version of the entropy related to the Einsteinian class of black objects with the following structure

$$S = \frac{\varpi_2 r_+^2}{4g^2(\varepsilon)} \left(\frac{b}{r_+}\right)^{2\gamma}, \quad (21)$$

in which by setting $\alpha = 0$ and $g(\varepsilon) = 1$, the entropy of Einstein-Maxwell-dilation black holes is recovered. In order to find the total electric charge of the solutions, one can use the Gauss law. Calculating the flux of electric field helps us to find the total electric charge with the following form

$$Q = \frac{\varpi_2 q f(\varepsilon)}{4\pi g(\varepsilon)}. \quad (22)$$

Next, we are interested in obtaining the electric potential. Using following standard relation, one can obtain the electric potential at the event horizon with respect to the infinity as a reference

$$U(r) = A_\mu \chi^\mu|_{r \rightarrow \infty} - A_\mu \chi^\mu|_{r \rightarrow r_+} = -\frac{2q}{r_+^3}. \quad (23)$$

Finally, according to the definition of mass due to Abbott and Deser [132–134], the total mass of the solution is

$$M = \frac{\varpi_2 b^{2\gamma}}{8\pi \mathcal{K}_{1,1} g(\varepsilon) f(\varepsilon)} m. \quad (24)$$

It is worthwhile to mention that for limiting case of $g(\varepsilon) = f(\varepsilon) = 1$ and $\alpha = 0$, Eq. (24) reduces to mass of the Einstein-Maxwell black holes [130]. In addition, in obtained conserved and thermodynamical quantities, only the electric potential remains unaffected by considering gravity's rainbow.

Now, we are in a position to check the validity of the first law of thermodynamics. To do so, first, we calculate the geometrical mass, m , by using $f(r = r_+) = 0$. Then by employing obtained relation for geometrical mass and Eq. (24) for total mass of the black holes, we find

$$M(r_+, q) = \frac{\varpi_2 A b^{2\gamma}}{8\pi \mathcal{K}_{1,-1} g(\varepsilon) f(\varepsilon)}, \quad (25)$$

where

$$A = \left(\frac{b}{r_+}\right)^{2\gamma} \left[k r_+^{\frac{\kappa_{1,-1}}{\kappa_{1,1}}} - q^2 f^2(\varepsilon) \mathcal{K}_{-1,1} r_+^{\frac{-\kappa_{1,3}}{\kappa_{1,1}}} + \frac{\Lambda \mathcal{K}_{1,1} \mathcal{K}_{1,-1}}{g^2(\varepsilon) \mathcal{K}_{-3,1}} r_+^{\frac{\kappa_{3,1}}{\kappa_{1,1}}} \left(\frac{b}{r_+}\right)^{4\gamma} \right].$$

It is a matter of calculation to show that

$$\left(\frac{\partial M}{\partial S}\right)_Q = T \quad \& \quad \left(\frac{\partial M}{\partial Q}\right)_S = U. \quad (26)$$

Therefore, we proved that the first law is valid as

$$dM = \left(\frac{\partial M}{\partial S}\right)_Q dS + \left(\frac{\partial M}{\partial Q}\right)_S dQ. \quad (27)$$

IV. THERMAL STABILITY

In this section, we study thermal stability of the solutions in context of the canonical ensemble. The stability conditions in the context of canonical ensemble are determined by the sign of the heat capacity. In other words, the positivity/negativity of the heat capacity is denoted as the black object being in stable/unstable state. Therefore, in order to study the stability of the charged black holes in dilatonic gravity's rainbow, we study the changes in the sign of corresponding heat capacity. It is worthwhile to mention that investigating the behavior of the heat capacity enables one to obtain the phase transitions of the solutions at the same time. The root and divergence point of the heat capacity are denoted as bounded point (r_{+0}) and second order phase transition point (r_{+c}), respectively. Bounded point is related to the root of temperature and the sign of T changes at r_{+0} , while we expect to obtain positive temperature at r_{+c} .

The system in canonical ensemble is considered to be in fixed charge. Therefore, we have

$$C_Q = \left(\frac{\partial M}{\partial S}\right)_Q \left(\frac{\partial^2 M}{\partial S^2}\right)_Q^{-1}. \quad (28)$$

Considering the mentioned bounded and phase transition points, one can obtain

$$\begin{cases} T = \left(\frac{\partial M}{\partial S}\right)_Q = 0 & \text{bounded point} \\ \left(\frac{\partial T}{\partial S}\right)_Q = \left(\frac{\partial^2 M}{\partial S^2}\right)_Q = 0 & \text{phase transition point} \end{cases}. \quad (29)$$

There are three valuable known cases for the rainbow functions which are characteristics of the rainbow solutions. These three cases are arisen from different phenomenological origins with an upper limit for considering the energy of test particle E

$$\varepsilon = \frac{E}{E_P} \leq 1.$$

The first case is originated from loop quantum gravity and non-commutative geometry. In this case, we have following relations for rainbow functions of metric [23, 24]

$$f(\varepsilon) = 1, \quad g(\varepsilon) = \sqrt{1 - \eta\varepsilon^n}. \quad (30)$$

The other case is constructed by considering the hard spectra from gamma-ray bursts which leads to [16]

$$f(\varepsilon) = \frac{e^{\beta\varepsilon} - 1}{\beta\varepsilon}, \quad g(\varepsilon) = 1. \quad (31)$$

Interestingly, opposite to previous case, in this one the effect of $g(\varepsilon)$ which is coupled to spatial coordinates of the metric is vanished, whereas in the case one which is related to loop quantum gravity the effect of coupling term for time component of the metric is vanished.

Finally, in the case three, the choices of rainbow functions are due to constancy of the velocity of the light [135]

$$f(\varepsilon) = g(\varepsilon) = \frac{1}{1 - \lambda\varepsilon}. \quad (32)$$

Using first law of thermodynamics, one can rewrite the relation for heat capacity into

$$C_Q = T \left(\frac{\partial S}{\partial r_+} \right)_Q \left(\frac{\partial T}{\partial r_+} \right)_Q^{-1}. \quad (33)$$

Now, by employing Eqs. (20) and (21) with (33), one can show that heat capacity is

$$C_Q = \frac{r_+^2 \left(\frac{b}{r_+} \right)^{2\gamma} \left(q^2 \mathcal{K}_{-1,1} g^2(\varepsilon) f^2(\varepsilon) + r_+^2 k g^2(\varepsilon) + r_+^4 \Lambda \mathcal{K}_{-1,1} \left(\frac{b}{r_+} \right)^{4\gamma} \right)}{2g^2(\varepsilon) \mathcal{K}_{-1,1} \left(r_+^2 k g^2(\varepsilon) - q^2 \mathcal{K}_{3,1} g^2(\varepsilon) f^2(\varepsilon) - r_+^4 \Lambda \mathcal{K}_{-1,1} \left(\frac{b}{r_+} \right)^{4\gamma} \right)}. \quad (34)$$

Considering obtained relation for the heat capacity (Eq.(34)) and three mentioned cases for the rainbow functions of the metric (Eqs. (30-32)), we study the stability of the solutions. In case of horizon flat ($k = 0$), one can find that the root(s) of the heat capacity and divergence point(s) are given by following relations

$$r_{+0} = b \left(-\frac{b^4 \Lambda}{g^2(\varepsilon) f^2(\varepsilon) q^2} \right)^{-\frac{\kappa_{1,1}}{4}}, \quad (35)$$

$$r_{+c} = b \left(-\frac{b^4 \Lambda \mathcal{K}_{-1,1}}{g^2(\varepsilon) f^2(\varepsilon) q^2 \mathcal{K}_{3,1}} \right)^{-\frac{\kappa_{1,1}}{4}}. \quad (36)$$

Interestingly, for horizon flat, the root of the heat capacity, hence bound point is independent of the dilaton parameter, α while divergency of the heat capacity is a function of this parameter. On the other hand, in order to have positive real valued divergency in AdS spacetime, we have $\alpha > 1$ restriction for dilaton parameter. This condition for dS spacetime is opposite. In other words, the real valued divergency is obtained if $0 \leq \alpha < 1$. (see Eqs. (35) and (36) for more details). In order to charged black holes in dilatonic gravity's rainbow with flat horizon be stable, following conditions must be hold

$$\left\{ \begin{array}{l} -\Lambda r_+^4 \left(\frac{b}{r_+} \right)^{6\gamma} \leq q^2 g(\varepsilon)^2 f(\varepsilon)^2 \left(\frac{b}{r_+} \right)^{2\gamma} \\ -\Lambda r_+^4 \mathcal{K}_{-1,1} \mathcal{K}_{1,1} \left(\frac{b}{r_+} \right)^{2\gamma} \leq q^2 g(\varepsilon)^2 f(\varepsilon)^2 \mathcal{K}_{3,1} \left(\frac{b}{r_+} \right)^{-2\gamma} \end{array} \right. .$$

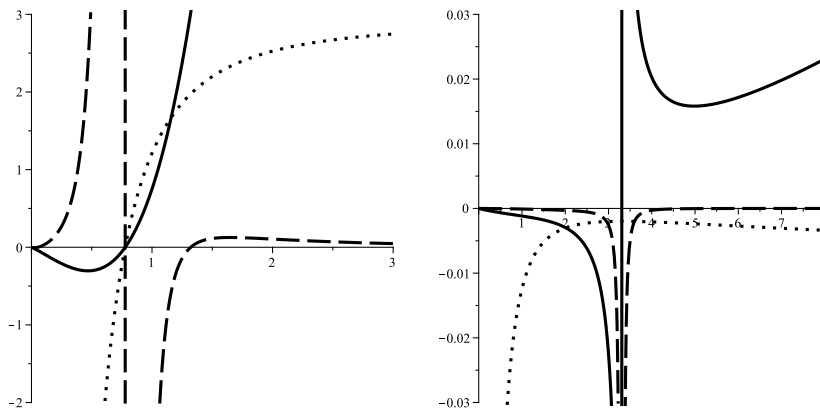


FIG. 2: C_Q (continuous line), T (dotted line) and \mathcal{R} (dashed line) versus r_+ for $k = 1$, $\Lambda = -1$, $b = 5$, $E = 1$, $E_p = 5$ and $q = 1$. $\alpha = 0.9$ (left panel) and $\alpha = 1.09$ (right panel) "different scales".

As for the cases of $k = \pm 1$, it was not possible to obtain the analytical relations for the root and divergence point of the heat capacity. Therefore, we employ numerical method for studying the properties of the heat capacity for spherical and hyperbolic horizons. As for the stability conditions, there are different orders of the horizon radius for each term. These terms will have dominant effect in specific regions of horizon radius and other parameters. Considering the effectiveness of these terms, the stability conditions will vary from one case to another one. Also, these effective behaviors may present different regions of stability and instability. Taking a closer look at different terms, one can see that the most effective parameter in stability conditions which modifies the exponent of horizon radius highly and changes the positivity and negativity of each term, is dilaton parameter, α . In other words, considering different values of α , stable/unstable regions will be modified highly. This highlights the effect of dilaton field on thermodynamical behavior of the solutions.

In order to give a better insight regarding the thermodynamical behavior of these black holes, we study the behavior of the temperature. The reason is the fact that negativity of the temperature represents nonphysical systems which are not of our interest. Therefore, we study the conditions for positivity/negativity of the temperature. Considering Eq. (20), there are three terms which are related to electric charge, cosmological constant and topological structure of the metric. The effectiveness of each term is a function of their factors. Therefore, considering different values for these factors may lead to one of the following scenarios: one root and temperature is an increasing function of horizon radius (left panel of Fig. 2), no root and temperature is negative with one maximum (right panel of Fig. 2), two roots with one region of positivity and two regions of negativity (Fig. 3), one root and temperature is a decreasing function of the horizon radius (Fig. 4).

In general, charged term is always negative in Eq. (20). If one considers AdS solutions, the second term will be positive. As for the last term, if spherical solution is chosen, then in order for topological term be positive, the dilaton parameter must be $\alpha > 1$. Whereas in case of hyperbolic horizon the condition will be modified into $\alpha < 1$. On the other hand, if dS solutions are considered, the second term will be negative. Therefore, the possibility of having positive temperature depends on topological term with mentioned conditions for spherical and hyperbolic cases. It is worthwhile to mention that horizon flat of dS solutions has negative temperature. Therefore, it is not physical. Considering the mentioned changes in different terms of temperature, depending on the dominant regions of the different each term, the temperature will have positive/negative value with different behavior (which were pointed out in plotted diagrams).

In order to elaborate the effects of the dilation field on thermal stability and mentioned behaviors for the temperature, we plot various diagrams using the first model of rainbow functions of gravity's rainbow.

It is evident that in case of temperature being an increasing function of horizon radius, for positive temperature, we have stable black holes and heat capacity is an increasing function of r_+ (Fig. 2 left panel). Increasing the dilaton parameter will lead to formation of two stable and unstable states where both of these states are in negative temperature (Fig. 2 right panel). On the other hand, by increasing dilaton parameter, the temperature will have two regions of negativity and one positivity. In the positive region, a phase transition takes place between unstable larger state to smaller stable state. This phase transition point is represented by a divergency of the heat capacity. Increasing dilaton parameter leads to decreasing the place of divergency of the heat capacity and increasing the region in which we have unstable physical solutions (Fig. 3). The larger root of the temperature is highly sensitive to variation of the α (see Fig. 3). For sufficiently large values of the dilaton parameter, the temperature is a decreasing

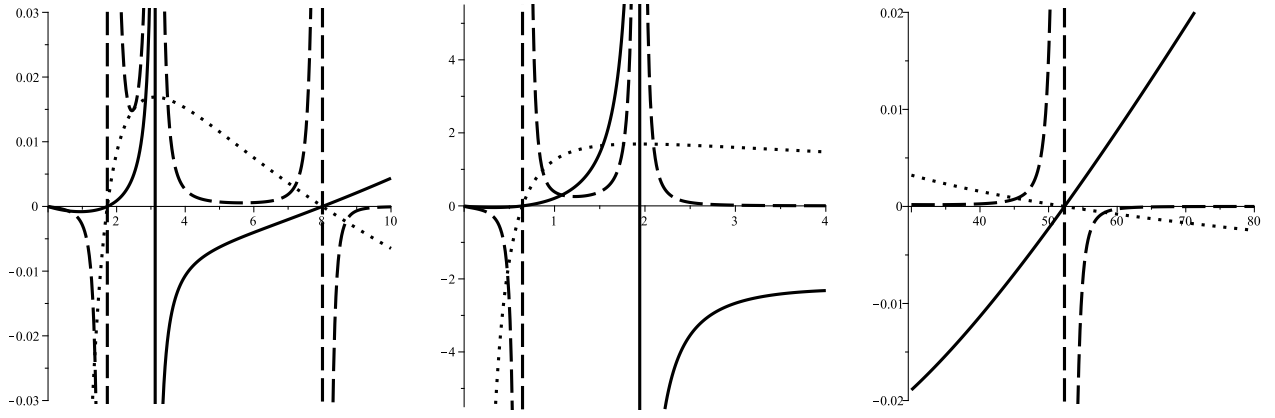


FIG. 3: C_Q (continuous line), T (dotted line) and \mathcal{R} (dashed line) versus r_+ for $k = 1$, $\Lambda = -1$, $b = 5$, $E = 1$, $E_p = 5$ and $q = 1$. $\alpha = 1.1$ (left panel) and $\alpha = 1.3$ (middle and right panels) "different scales".

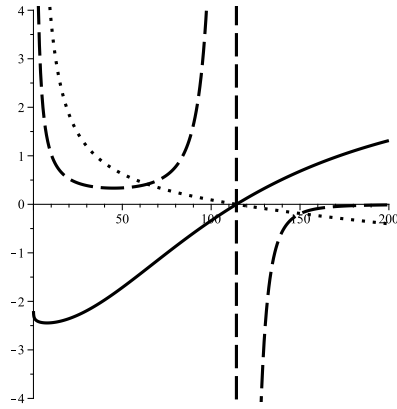


FIG. 4: C_Q (continuous line), T (dotted line) and \mathcal{R} (dashed line) versus r_+ for $k = 1$, $\Lambda = -1$, $b = 5$, $E = 1$, $E_p = 5$ and $q = 1$. $\alpha = 10$ (left panel) and $\alpha = 15$ (right panel) "different scales".

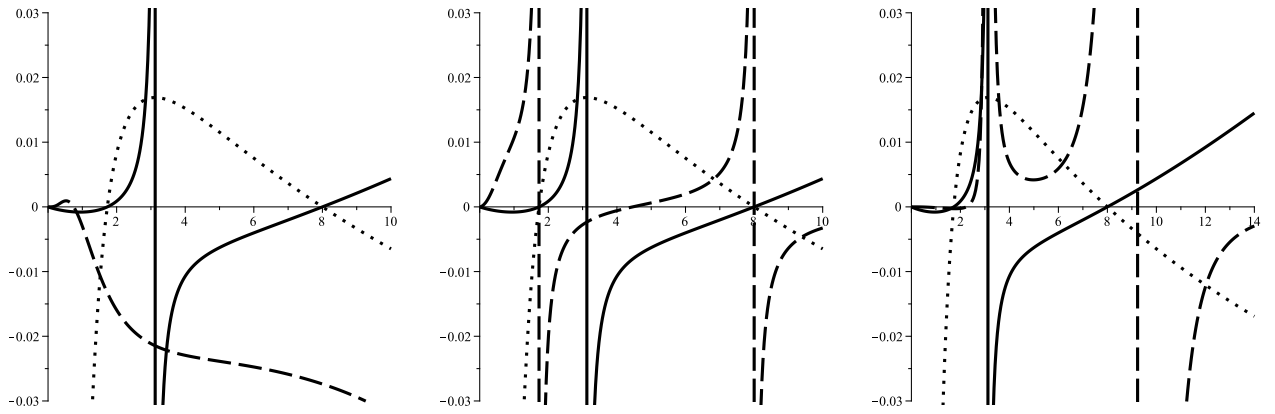


FIG. 5: C_Q (continuous line), T (dotted line) and \mathcal{R} (dashed line) versus r_+ for $k = 1$, $\Lambda = -1$, $b = 5$, $E = 1$, $E_p = 5$, $q = 1$ and $\alpha = 1.1$. Weinhold (left panel), Ruppeiner (middle panel) and Quevedo (middle panel) "different scales".

function of the horizon radius with one root. The heat capacity in the region of the positive temperature is negative, therefore in this case rainbow solutions are unstable (Fig. 4). It is worthwhile to mention that the root in this case is an increasing function of dilaton parameter (compare two diagrams of Fig. 4).

V. GEOMETRICAL THERMODYNAMICS

In this section, we will conduct a study regarding the phase transition points of the obtained black holes through the use of geometrical thermodynamics concept. In this concept, one can construct the thermodynamical structure of the black hole through the use of thermodynamical variables. In other words, by using one of the thermodynamical variable as potential and its corresponding extensive parameters, it is possible to build phase space. The singularities of the Ricci scalar of this phase space, marks two different properties of the solutions: one is a bound point which is related to the root of the temperature and marks the physical and non-physical solutions. The other one is related to singularities of the heat capacity which are marking the points which system goes under phase transition.

Considering such property for the constructed phase space, a valid approach of the geometrical thermodynamics produces a Ricci scalar which has singularities that cover both of the mentioned points. Depending on the thermodynamical potential, the extensive parameters would be different for each phase space. One of these potentials could be entropy which could be used to construct Ruppeiner phase space. An other potential could be mass which is employed to build Weinhold, Quevedo and HPEM phase spaces. The mentioned phase spaces have following forms [115–117]

$$ds^2 = \begin{cases} Mg_{ab}^W dX^a dX^b & \text{Weinhold} \\ -MTg_{ab}^W dX^a dX^b & \text{Ruppeiner} \\ (SM_S + QM_Q) (-M_{SS}dS^2 + M_{QQ}dQ^2) & \text{Quevedo} \\ S \frac{M_S}{M_{SQ}^3} (-M_{SS}dS^2 + M_{QQ}dQ^2) & \text{HPEM} \end{cases}, \quad (37)$$

where their corresponding denominator of their Ricci scalars are

$$\text{denom}(\mathcal{R}) = \begin{cases} (M_{SS}M_{QQ} - M_{SQ}^2)^2 M^2(S, Q) & \text{Weinhold} \\ (M_{SS}M_{QQ} - M_{SQ}^2)^2 T(S, Q)M^2(S, Q) & \text{Ruppeiner} \\ (SM_S + QM_Q)^3 M_{SS}^2 M_{QQ}^2 & \text{Quevedo} \\ S^3 M_S^3 M_{SS}^2 & \text{HPEM} \end{cases}, \quad (38)$$

in which $M_{QQ} = \left(\frac{\partial^2 M}{\partial Q^2}\right)_S$, $M_{SQ} = \frac{\partial^2 M}{\partial S \partial Q}$, $M_{SS} = \left(\frac{\partial^2 M}{\partial S^2}\right)_Q$ and $M_S = \left(\frac{\partial M}{\partial S}\right)_Q$.

Now, by using Eqs. (21), (22), (25) and (37), one can construct mentioned phase spaces and calculate their corresponding curvature scalar for these black holes. Due to economical reasons, we will not present obtained relation for Ricci scalar but demonstrate results in plotted diagrams (see Figs. 2-4 for HPEM metric and Fig. 5 for other metrics). Fig. 5 shows that for specific values one can find cases in which Weinhold (left panel of Fig. 5), Ruppeiner (middle panel of Fig. 5) and Quevedo (right panel Fig. 5) will not produce suitable divergencies in their Ricci scalar to cover mentioned points. In other words, the divergencies of their Ricci scalar may not coincide with root and divergencies of the heat capacity. On the other hand, it is seen that all the divergencies of the curvature scalar of the HPEM metric match with bound and phase transition points of the heat capacity. The nature of the behavior of the Ricci scalar around each one of these divergencies enables one to recognize whether it is a bound point or a divergence point in heat capacity [115–117].

VI. PHASE TRANSITIONS IN EXTENDED PHASE SPACE

In this section, we investigate the existence of second order phase transition through the analogy between negative cosmological constant and thermodynamical pressure. The usual relation for pressure and cosmological constant is

give by [99–101, 136]

$$P = -\frac{\Lambda}{8\pi}. \quad (39)$$

It was shown that the gravitational theory under consideration may affect this relation and modifies it [137, 138]. In calculations of the conserved and thermodynamical quantities, we found that these quantities were modified due to existence of gravity's rainbow and dilaton field. It is natural to question whether the usual relation between cosmological constant and thermodynamical pressure could be modified in presence of the dilaton field as well as rainbow functions. To investigate such modification, we use the right hand side of the Eq. (7). It is a matter of calculation to show that (after removing parts related to electromagnetic field)

$$T_r^r \propto \Lambda \left(\frac{b}{r_+} \right)^{2\gamma}. \quad (40)$$

Obtained relation indicates that although both dilaton field and rainbow functions modified thermodynamical quantities, only the dilatonic part has direct effect on the relation between cosmological constant and pressure. Therefore, we use following analogy for studying the critical behavior of the system

$$P = -\frac{\Lambda}{8\pi} \left(\frac{b}{r_+} \right)^{2\gamma}. \quad (41)$$

The conjugating quantity related to pressure is obtained through the use of enthalpy

$$V = \left(\frac{\partial H}{\partial P} \right)_T. \quad (42)$$

Since consideration of the cosmological constant extends our thermodynamical phase space, the mass term plays the role of enthalpy. Therefore, by using Eqs. (24), (41) and (42), one can find modified volume of these dilatonic black holes as

$$V = \frac{\mathcal{K}_{1,1}}{\mathcal{K}_{3,-1} g^3(\varepsilon) f(\varepsilon)} r_+^{\frac{\kappa_{5,3}}{\kappa_{1,1}}} b^{2\gamma}. \quad (43)$$

Clearly, the volume of these black holes is a function of both rainbow functions and dilaton parameter. In other words, contrary to some specific modified gravities, in this gravity, the volume of the black hole is affected by the presence of rainbow and dilaton gravities. Here, in order to have a positive and non-zero volume, we find a restriction $-3 < \alpha < 3$. Since we are not interested in negative values of the α , we restrict ourselves to $0 < \alpha < 3$.

It should be pointed out that due to the relation between volume of the black hole and horizon radius, one is able to introduce specific volume for these black holes which enables us to use horizon radius instead of volume in following calculations. So, the pressure is given by

$$P = \frac{\mathcal{K}_{3,-1} g(\varepsilon) f(\varepsilon) \left(\frac{b}{r_c} \right)^{2\gamma} r_+^{\frac{\kappa_{-1,1}}{\kappa_{1,1}}} b^{-2\gamma}}{2\mathcal{K}_{1,1} \mathcal{K}_{3,1}} T + \frac{\mathcal{K}_{3,-1} g^2(\varepsilon) [f^2(\varepsilon) \mathcal{K}_{-1,1} q^2 + r_+^2]}{8r_+^4 \pi \mathcal{K}_{-1,1} \mathcal{K}_{3,1}} \left(\frac{b}{r_+} \right)^{-2\gamma}. \quad (44)$$

In order to find a relation for calculating critical volume, hence critical horizon radius, we use the concept of inflection point. In this method, one uses

$$\left(\frac{\partial P}{\partial r_+} \right)_T = \left(\frac{\partial^2 P}{\partial r_+^2} \right)_T = 0,$$

to find critical horizon radius which in case of this thermodynamical system is

$$r_c = qf(\varepsilon) \sqrt{\mathcal{K}_{3,1} \mathcal{K}_{2,1}}, \quad (45)$$

which will lead to following critical temperature and pressure

$$T_c = \frac{\mathcal{K}_{1,1} g(\varepsilon) r_c^{\frac{\kappa_{1,-1}}{\kappa_{1,1}}} b^{2\gamma}}{f^3(\varepsilon) q^2 \pi \mathcal{K}_{1,-1} \mathcal{K}_{2,1}^2 \mathcal{K}_{3,1}^2} \left(\frac{b}{r_c} \right)^{-4\gamma}, \quad (46)$$

$$(47)$$

$$P_c = \frac{g^2(\varepsilon) \mathcal{K}_{3,-1} \left(\frac{b}{r_c} \right)^{-2\gamma}}{8\pi f^2(\varepsilon) q^2 \mathcal{K}_{3,1} \mathcal{K}_{2,1}}. \quad (48)$$

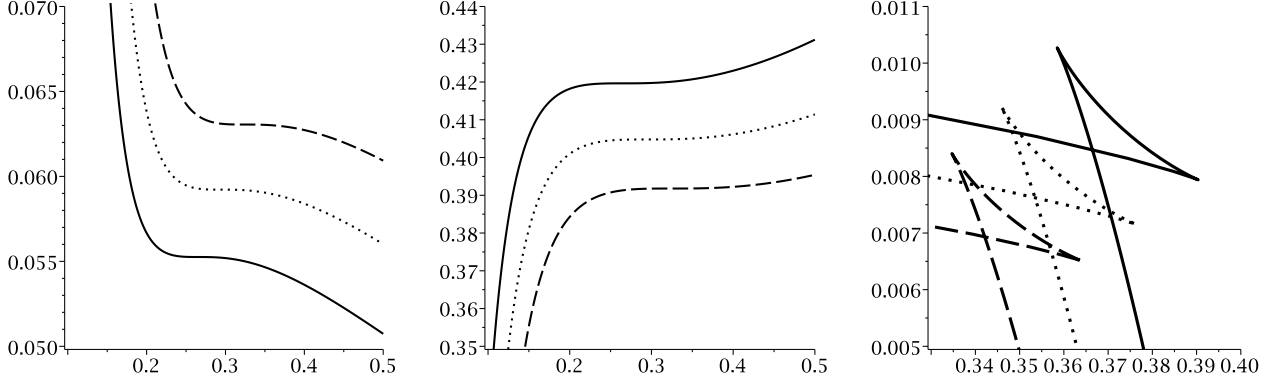


FIG. 6: $P - r_+$ (left), $T - r_+$ (middle) and $G - T$ (right) diagrams for $q = 0.1$, $b = 1$, $\alpha = 0.7$, $g(\varepsilon) = f(\varepsilon) = 0.9$ (continuous line), $g(\varepsilon) = f(\varepsilon) = 1$ (dotted line) and $g(\varepsilon) = f(\varepsilon) = 1.1$ (dashed line). $P - r_+$ diagram for $T = T_c$, $T - r_+$ diagram for $P = P_c$ and $G - T$ diagram for $P = 0.5P_c$.

It is worthwhile to mention that the restriction that was observed was originated only from dilatonic part of the solutions. In other words, we have no restriction on values that charge and rainbow functions can acquire and our system is only thermodynamically restricted by dilaton parameter.

Using obtained critical values, one can find the following critical ratio

$$\frac{P_c r_c}{T_c} = \frac{qg(\varepsilon)f^2(\varepsilon)\mathcal{K}_{-1,1}\mathcal{K}_{3,1}^{1/2}}{8\mathcal{K}_{1,1}\mathcal{K}_{2,1}^{1/2}} \left(\frac{b}{r_c}\right)^{2\gamma} r_c^{\frac{\kappa_{1,-1}}{\kappa_{1,1}}} b^{2\gamma}, \quad (49)$$

which shows that this critical ratio was modified due to the presence of dilaton field as well as rainbow functions. It is worthwhile to mention that critical horizon radius depends only on one of the rainbow functions whereas the other critical values and also the ratio $\frac{P_c r_c}{T_c}$ are functions of both of them. In addition, it is notable that in the absence of dilaton field ($\alpha = 0$) and low energy limit ($f(\varepsilon) = g(\varepsilon) = 1$), Eq. (49) reduces to the usual universal ratio in four dimensional Einstein gravity [95, 99].

Next, using the renewed role of the total mass of the black holes, we have Gibbs free energy as

$$G = H - TS = M - TS, \quad (50)$$

which by using Eqs. (20), (21), (24) and (41) will be

$$G = \frac{\mathcal{K}_{1,1}^2 b^{2\gamma} r_+^{\frac{\alpha^2+3}{\kappa_{1,1}}}}{2\mathcal{K}_{-3,1} f(\varepsilon) g^3(\varepsilon)} P + \frac{\mathcal{K}_{3,1} f(\varepsilon) \left(\frac{b}{r_c}\right)^{-2\gamma} r_c^{-\frac{\kappa_{1,3}}{\kappa_{1,1}}} b^{2\gamma}}{16\pi g(\varepsilon)} q^2 + \frac{\left(\frac{b}{r_c}\right)^{-2\gamma} r_c^{\frac{\kappa_{1,-1}}{\kappa_{1,1}}} b^{2\gamma}}{16\pi f(\varepsilon) g(\varepsilon)}. \quad (51)$$

In order to see whether obtained critical values represent a second order phase transition, we study phase diagrams ($P - r_+$, $T - r_+$ and $G - T$ diagrams) in Figs. 6-8.

It is evident that for specific values of different parameters, a second order phase transition is observed for obtained critical values (see Figs. 6 and 7). The critical pressure (left panels of Figs. 6 and 7), temperature and subcritical isobars (middle panels of Figs. 6 and 7), energy of different phases and size of swallow-tails (right panels of Figs. 6 and 7) are functions of gravity's rainbow and dilaton parameter. The effects of rainbow functions and dilaton parameter on critical values are different from each other (compare Figs. 6 with 7).

Interestingly, for a set of values, it is possible to obtain positive critical pressure and horizon radius whereas the temperature is negative. The plotted diagrams for these cases show a normal critical behavior in $P - r_+$ diagram (left panel of Fig. 8) whereas in $G - T$ diagram an abnormal behavior is observed (right panel of Fig. 8). In case of $T - r_+$ diagram, also normal critical behavior is observed except that this behavior is located in negative temperature.

VII. PHASE TRANSITION POINTS THROUGH HEAT CAPACITY

In this section, we will obtain critical points through a method which was developed in Ref. [104]. In this method, the denominator of the heat capacity is employed to obtain an explicit relation for thermodynamical pressure. Obtained

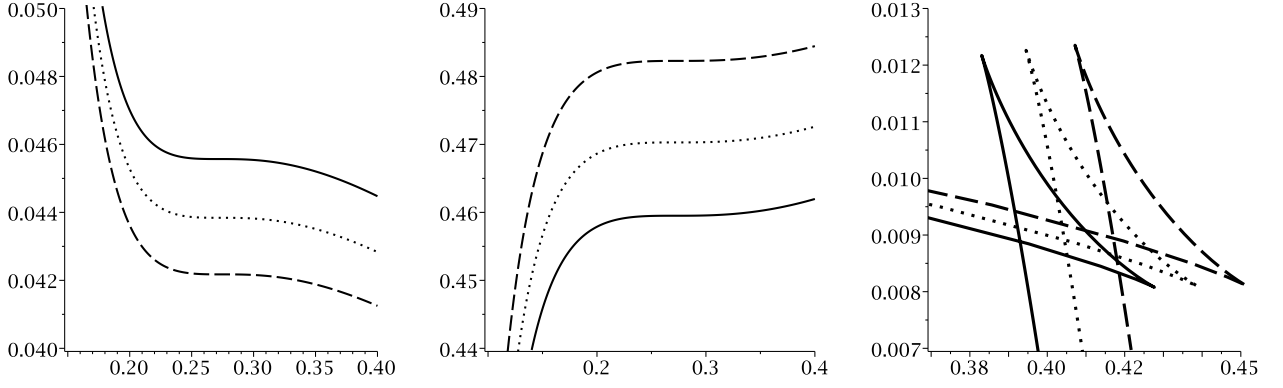


FIG. 7: $P - r_+$ (left), $T - r_+$ (middle) and $G - T$ (right) diagrams for $q = 0.1$, $b = 1$, $g(\varepsilon) = f(\varepsilon) = 0.9$, $\alpha = 0.75$ (continuous line), $\alpha = 0.76$ (dotted line) and $\alpha = 0.77$ (dashed line).
 $P - r_+$ diagram for $T = T_c$, $T - r_+$ diagram for $P = P_c$ and $G - T$ diagram for $P = 0.4P_c$.

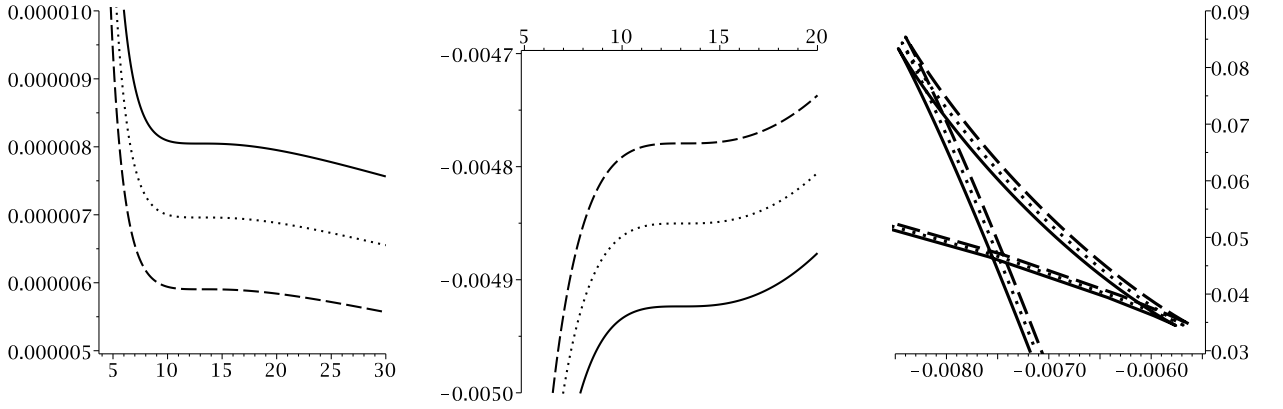


FIG. 8: $P - r_+$ (left), $T - r_+$ (middle) and $G - T$ (right) diagrams for $q = 1$, $b = 20$, $g(\varepsilon) = f(\varepsilon) = 2.5$, $\alpha = 0.75$ (continuous line), $\alpha = 0.76$ (dotted line) and $\alpha = 0.77$ (dashed line).
 $P - r_+$ diagram for $T = T_c$, $T - r_+$ diagram for $P = P_c$ and $G - T$ diagram for $P = 0.5P_c$.

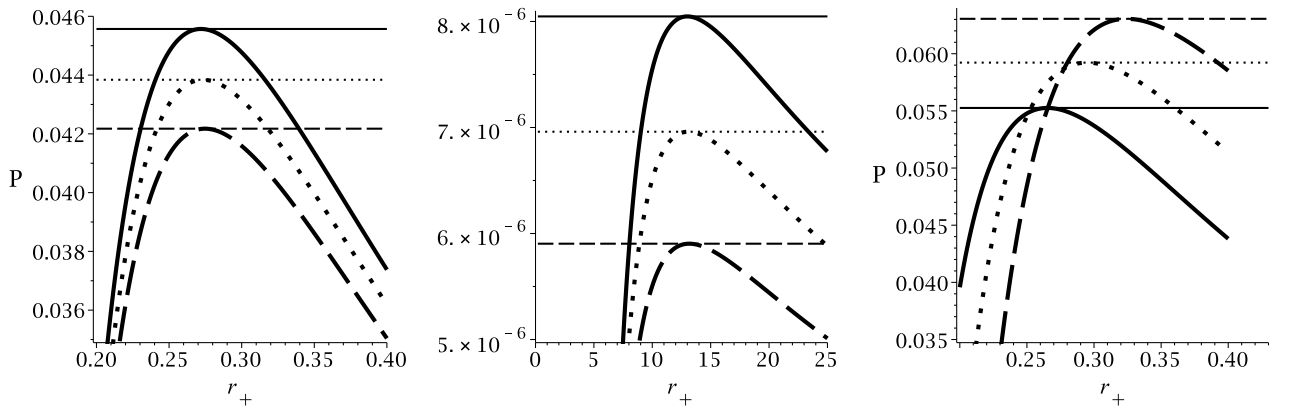


FIG. 9: P versus r_+ diagrams for $q = 0.1$, $b = 1$ and $k = 1$.
left panel: $g(\varepsilon) = f(\varepsilon) = 0.9$ and $\alpha = 0.75$ (bold continuous line), $P = 0.0455693$ (continuous line), $\alpha = 0.76$ (bold dotted line), $P = 0.0438404$ (dotted line), $\alpha = 0.77$ (bold dashed line), $P = 0.0421757$ (dashed line).
middle panel: $g(\varepsilon) = f(\varepsilon) = 0.9$ and $\alpha = 1.65$ (bold continuous line), $P = 0.0000080$ (continuous line), $\alpha = 1.66$ (bold dotted line), $P = 0.0000069$ (dotted line), $\alpha = 1.67$ (bold dashed line), $P = 0.0000059$ (dashed line).
right panel: $\alpha = 0.7$ and $g(\varepsilon) = f(\varepsilon) = 0.9$ (bold continuous line), $P = 0.0552557$ (continuous line), $g(\varepsilon) = f(\varepsilon) = 1$ (bold dotted line), $P = 0.0592206$ (dotted line), $g(\varepsilon) = f(\varepsilon) = 1.1$ (bold dashed line), $P = 0.0630518$ (dashed line).

relation may yield a maximum(s) for pressure which is(are) critical pressure(s) in which a second order phase transition takes place. This critical pressure is exactly the same as that of obtained through the use of phase diagrams.

Using Eqs. (34) and (41) and solving the denominator with respect to thermodynamical pressure will lead to following explicit relation for pressure

$$P = \frac{\mathcal{K}_{-3,1} [q^2 f^2(\varepsilon) \mathcal{K}_{3,1} - r_+^2] g^2(\varepsilon)}{8\pi r_+^4 \mathcal{K}_{3,1} \mathcal{K}_{1,1}} \left(\frac{b}{r_+} \right)^{-2\gamma}. \quad (52)$$

It is evident that this relation is different from previously obtained relation for pressure (Eq. 44). Now, by using values that are employed for plotting phase diagrams (Figs. 6-8), we plot following diagrams (Fig. 9). A simple comparison shows that the maximums of the plotted diagrams are exactly where corresponding critical pressure and horizon radius are located in phase diagrams. This shows that these two approaches yield consisting picture regarding the critical behavior of these black holes. On the other hand, plotted diagram which corresponds to one with abnormal behavior (middle panel of Fig. 9) also represents the characteristic behavior of the phase transition point. Therefore, in case of these black holes, a phase transition occurs in the mentioned critical point.

VIII. CONCLUSION

In this paper, we studied 4-dimensional charged dilatonic black holes in gravity's rainbow and their thermal stability conditions. We obtained thermodynamical quantities such as temperature, electric charge, entropy and total mass of the black holes. These quantities were modified in gravity's rainbow and became energy dependent.

Next, we conducted a study regarding physical/nonphysical black holes (positivity/negativity of temperature) and thermal stability of the solutions. It was pointed out that dominant factor in studying these properties is the dilaton parameter. In other words, these properties were highly sensitive to variation of α . Due to different factors of dilaton parameter, different types of behavior were observed for temperature which put restrictions on the solutions being physical. Observed behaviors for the temperature were: a) two roots with maximum, b) an increasing (a decreasing) function of horizon radius with one root c) a negative definite function with one maximum.

The analyzed behaviors were, increasing function of horizon radius with one root, increasing and decreasing function of horizon radius with two roots, decreasing function of the r_+ with one root located and being negative with one maximum located at negative temperature.

As for the stability and phase transition, we found depending on the behavior of the temperature, heat capacity could have phase transition and stable state for larger values of horizon radius. In case of two roots for temperature, interestingly, a phase transition of larger/smaller black hole was observed. Finally, as for temperature being decreasing function of r_+ , for physical solutions (positive temperature), unstable solutions were observed. In other words, in this case, physical solutions are unstable.

Next, geometrical approach was employed to study the bound and phase transition points of these black holes. It was demonstrated that the Ricci scalars of the phase spaces of Weingold, Ruppeiner and Quevedo metrics, have divergencies which do not match with mentioned points while the singular points of curvature scalar of the HPEM coincide with roots and divergence points of the heat capacity.

We also, studied the critical behavior of these black holes in extended phase space. It was shown that the usual relation between cosmological constant and thermodynamical pressure was modified due to existence of dilaton gravity whereas such modification was not seen for gravity's rainbow. On the contrary, it was shown that volume of the black holes depends on both of these modifications.

Then, we showed that the critical values are related to the rainbow functions as well as the dilaton parameter. In order to have positive critical temperature, we found restrictions which were purely dilatonic dependant. Therefore, one is not free to choose any value for dilaton parameter.

In studying phase diagrams, two different behaviors were observed for different diagrams, especially in $G - T$ diagrams. Interestingly, although we observed an anomaly in these diagrams, other corresponding phase diagrams presented usual thermodynamical behavior around critical points. In other words, the observed abnormal behaviors in phase diagrams present the existence of a second order phase transition for these black holes.

Next, we used a new method which was introduced in Ref. [104], for studying the critical behavior of the system. This method is based on obtaining an explicit form for thermodynamical pressure from denominator of the heat capacity. It was seen that the maximum maximum of this relation is located at the critical pressure and horizon radius in which second order phase transition takes place. It was shown that in this method, for irregular behavior which was observed in phase diagrams, also a second order phase transition occurs. This indicates that these points are phase transition point despite their abnormal behavior.

Finally, it is worthwhile to think about the physical interpretation of abnormal behavior which was seen in this paper. It is notable that, one can generalize obtained linear solutions in this paper to nonlinear case of electrodynamics

and investigate the effects of nonlinearity [139]. In addition, one may investigate the extended phase space and thermodynamic criticality in higher order Lovelock-Maxwell gravity's rainbow as well as Lovelock-nonlinear electrodynamics [140, 141]. These subjects are under examination.

Acknowledgments

We thank the Shiraz University Research Council. This work has been supported financially by the Research Institute for Astronomy and Astrophysics of Maragha, Iran.

-
- [1] P. Horava, Phys. Rev. D **79**, 084008 (2009).
 - [2] P. Horava, Phys. Rev. Lett. **102**, 161301 (2009).
 - [3] R. Gregory, S. L. Parameswaran, G. Tasinato and I. Zavala, JHEP **12**, 047 (2010).
 - [4] P. Burda, R. Gregory and S. Ross, JHEP **11**, 073 (2014).
 - [5] S. S. Gubser and A. Nellore, Phys. Rev. D **80**, 105007 (2009).
 - [6] Y. C. Ong and P. Chen, Phys. Rev. D **84**, 104044 (2011).
 - [7] M. Alishahiha and H. Yavartanoo, Class. Quantum Gravit. **31**, 095008 (2014).
 - [8] S. Kachru, N. Kundu, A. Saha, R. Samanta and S. P. Trivedi, JHEP **03**, 074 (2014).
 - [9] K. Goldstein, N. Iizuka, S. Kachru, S. Prakash, S. P. Trivedi and A. Westphal, JHEP **10**, 027 (2010).
 - [10] G. Bertoldi, B. A. Burrington and A. W. Peet, Phys. Rev. D **82**, 106013 (2010).
 - [11] M. Kord Zangeneh, A. Sheykhi and M. H. Dehghani, Phys. Rev. D **92**, 024050 (2015).
 - [12] J. Tarrio and S. Vandoren, JHEP **09**, 017 (2011).
 - [13] J. Magueijo and L. Smolin, Class. Quantum Gravit. **21**, 1725 (2004).
 - [14] R. Garattini and E. N. Saridakis, Eur. Phys. J. C **75**, 343 (2015).
 - [15] G. 't Hooft, Class. Quantum Gravit. **13**, 1023 (1996).
 - [16] G. Amelino-Camelia, J. R. Ellis, N. Mavromatos, D. V. Nanopoulos and S. Sarkar, Nature **393**, 763 (1998).
 - [17] R. Gambini and J. Pullin, Phys. Rev. D **59**, 124021 (1999).
 - [18] M. Faizal, J. Phys. A **44**, 402001 (2011).
 - [19] S. M. Carroll, J. A. Harvey, V. A. Kostelecky, C. D. Lane and T. Okamoto, Phys. Rev. Lett. **87**, 141601 (2001).
 - [20] M. Faizal, Mod. Phys. Lett. A **27**, 1250075 (2012).
 - [21] N. Seiberg and E. Witten, JHEP **09**, 032 (1999).
 - [22] Y. E. Cheung and M. Krogh, Nucl. Phys. B **528**, 185 (1998).
 - [23] G. Amelino-Camelia, Living Reviews in Relativity **5**, 16 (2013).
 - [24] U. Jacob, F. Mercati, G. Amelino-Camelia and T. Piran, Phys. Rev. D **82**, 084021 (2010).
 - [25] V. A. Kostelecky and S. Samuel, Phys. Rev. D **39**, 683 (1989).
 - [26] V. A. Kostelecky and S. Samuel, Phys. Rev. D **40**, 1886 (1989).
 - [27] S. Mukohyama, JHEP **05**, 048 (2007).
 - [28] P. West, Phys. Lett. B **548**, 92 (2002).
 - [29] R. Iengo, J. G. Russo and M. Serone, JHEP **11**, 020 (2009).
 - [30] A. Adams, N. Arkani-Hamed, S. Dubovsky, A. Nicolis and R. Rattazzi, JHEP **10**, 014 (2006).
 - [31] B. M. Gripaios, JHEP **10**, 069 (2004).
 - [32] J. Alfaro, P. Gonzalez and R. Avila, Phys. Rev. D **91**, 105007 (2015).
 - [33] H. Belich and K. Bakke, Phys. Rev. D **90**, 025026 (2014).
 - [34] A. F. Ali, M. Faizal and M. M. Khalil, JHEP **12**, 159 (2014).
 - [35] A. F. Ali, M. Faizal and M. M. Khalil, Nucl. Phys. B **894**, 341 (2015).
 - [36] A. F. Ali, Phys. Rev. D **89**, 104040 (2014).
 - [37] Y. Ling X. Li and H. B. Zhang, Mod. Phys. Lett. A **22**, 2749 (2007).
 - [38] H. Li, Y. Ling and X. Han, Class. Quantum Gravit. **26**, 065004 (2009).
 - [39] A. F. Ali, M. Faizal and B. Majumder, Europhys. Lett. **109**, 20001 (2015).
 - [40] Y. Gim and W. Kim, JCAP **05**, 002 (2015).
 - [41] A. F. Ali, M. Faizal and M. M. Khalil, Phys. Lett. B **743**, 295 (2015).
 - [42] R. Garattini and B. Majumder, Nucl. Phys. B **884**, 125 (2014).
 - [43] S. H. Hendi and M. Faizal, Phys. Rev. D **92**, 044027 (2015).
 - [44] Z. Chang and S. Wang, Eur. Phys. J. C **75**, 259 (2015).
 - [45] R. Garattini and B. Majumder, Nucl. Phys. B **883**, 598 (2014).
 - [46] G. Santos, G. Gubitosi and G. Amelino-Camelia, JCAP **08**, 005 (2015).
 - [47] A. F. Ali and M. M. Khalil, Europhys. Lett. **110**, 20009 (2015).
 - [48] S. H. Hendi, S. Panahiyan, B. Eslam Panah and M. Momennia, [arXiv:1512.05192].
 - [49] S. H. Hendi, G. H. Bordbar, B. Eslam Panah and S. Panahiyan, [arXiv:1509.05145].

- [50] E. Witten, Phys. Rev. D **44**, 314 (1991).
- [51] J. H. Horne and G. T. Horowitz, Nucl. Phys. B **368**, 444 (1991).
- [52] Y. M. Cho, Phys. Rev. D **41**, 2462 (1990).
- [53] Z. G. Huang, H. Q. Lu and W. Fang, Int. J. Mod. Phys. D **16**, 1109 (2007).
- [54] Z. G. Huang and X. M. Song, Astrophys. Space Sci. **315**, 175 (2008).
- [55] T. Tamaki and T. Torii, Phys. Rev. D **62**, 061501R (2000).
- [56] R. Yamazaki and D. Ida, Phys. Rev. D **64**, 024009 (2001);
- [57] S. S. Yazadjiev, Phys. Rev. D **72**, 044006 (2005).
- [58] P. P. Fiziev, [arXiv:1506.08585].
- [59] S. H. Hendi, G. H. Bordbar, B. Eslam Panah and M. Najafi, Astrophys. Space Sci. **358**, 30 (2015).
- [60] C. G. Callan, S. B. Giddings, J. A. Harvey and A. Strominger, Phys. Rev. D **45**, R1005 (1992).
- [61] T. Banks, A. Dabholkar, M. R. Douglas and M. O’Loughlin, Phys. Rev. D **45**, 3607 (1992).
- [62] S. W. Hawking, Commun. Math. Phys. **25**, 167 (1972).
- [63] J. D. Beckenstein, Phys. Rev. D **7**, 2333 (1973);
- [64] E. Witten, Adv. Theor. Math. Phys. **2**, 253 (1998).
- [65] J. M. Maldacena, Int. J. Theor. Phys. **38**, 1113 (1999).
- [66] O. Aharony, S. S. Gubser, J. M. Maldacena, H. Ooguri and Y. Oz, Phys. Rept. **323**, 183 (2000).
- [67] O. Aharony, O. Bergman, D. L. Jafferis and J. M. Maldacena, JHEP **10**, 091 (2008).
- [68] D. A. Lowe, Phys. Rev. D **79**, 106008 (2009).
- [69] J. Jing and S. Chen, Phys. Lett. B **686**, 68 (2010).
- [70] Y. P. Hu, P. Sun and J. H. Zhang, Phys. Rev. D **83**, 126003 (2011)
- [71] X. O. Camanho and J. D. Edelstein, JHEP **04**, 007 (2010).
- [72] Y. P. Hu, H. F. Li and Z. Y. Nie, JHEP **01**, 123 (2011).
- [73] J. Jing, Q. Pan and S. Chen, JHEP **11**, 045 (2011).
- [74] D. Bazeia, L. Losano, G. J. Olmo and D. Rubiera-Garcia, Phys. Rev. D **90**, 044011 (2014).
- [75] D. Kabat and G. Lifschytz, JHEP **09**, 077 (2014).
- [76] J. Polchinski, [arXiv:1010.6134].
- [77] I. R. Klebanov, [arXiv:hep-th/9901018].
- [78] D. T. Son and A. O. Starinets, Ann. Rev. Nucl. Part. Sci. **57**, 95 (2007).
- [79] S. W. Hawking and D. N. Page, Commun. Math. Phys. **87**, 577 (1983).
- [80] E. Witten, Adv. Theor. Math. Phys. **2**, 505 (1998).
- [81] Y. S. Myung, Phys. Rev. D **77**, 104007 (2008).
- [82] B. M. N. Carter and I. P. Neupane, Phys. Rev. D **72**, 043534 (2005);
- [83] D. Kastor, S. Ray and J. Traschen, Class. Quantum Gravit. **26**, 195011 (2009);
- [84] F. Capela and G. Nardini, Phys. Rev. D **86**, 024030 (2012).
- [85] S. H. Hendi, S. Panahiyan and H. Mohammadpour, Eur. Phys. J. C **72**, 2184 (2012).
- [86] S. H. Hendi, S. Panahiyan and E. Mahmoudi, Eur. Phys. J. C **74**, 3079 (2014).
- [87] S. H. Hendi and S. Panahiyan, Phys. Rev. D **90**, 124008 (2014).
- [88] A. Perez, M. Riquelme, D. Tempo and R. Troncoso, JHEP **10**, 161 (2015).
- [89] S. H. Hendi, S. Panahiyan and B. Eslam Panah, [arXiv:1507.06563] "accepted in JHEP".
- [90] A. Perez, M. Riquelme, D. Tempo and R. Troncoso, [arXiv:1512.01576].
- [91] G.W. Gibbons, R. Kallosh and B. Kol, Moduli, Phys. Rev. Lett. **77**, 4992 (1996).
- [92] J. D. E. Creighton and R. B. Mann, Phys. Rev. D **52**, 4569 (1995).
- [93] B. P. Dolan, Class. Quantum Gravit. **28**, 125020 (2011).
- [94] B. P. Dolan, Class. Quantum Gravit. **28**, 235017 (2011).
- [95] D. Kubiznak and R. B. Mann, JHEP **07**, 033 (2012).
- [96] R. G. Cai, L. M. Cao, L. Li and R. Q. Yang, JHEP **09**, 005 (2013).
- [97] M. B. Jahani Poshteh, B. Mirza and Z. Sherkatghanad, Phys. Rev. D **88**, 024005 (2013);
- [98] S. Chen, X. Liu and C. Liu, Chin. Phys. Lett. **30**, 060401 (2013).
- [99] S. H. Hendi and M. H. Vahidinia, Phys. Rev. D **88**, 084045 (2013).
- [100] J. X. Mo and W. B. Liu, Eur. Phys. J. C **74**, 2836 (2014);
- [101] D. C. Zou, S. J. Zhang and B. Wang, Phys. Rev. D **89**, 044002 (2014);
- [102] W. Xu and L. Zhao, Phys. Lett. B **736**, 214 (2014).
- [103] A. M. Frassino, D. Kubiznak, R. B. Mann and F. Simovic, JHEP **09**, 080 (2014).
- [104] S. H. Hendi, S. Panahiyan and B. Eslam Panah, Int. J. Mod. Phys. D **25**, 1650010 (2016).
- [105] J. Xu, L. M. Cao and Y. P. Hu, Phys. Rev. D **91**, 124033 (2015).
- [106] S. H. Hendi, S. Panahiyan and M. Momennia, [arXiv:1503.03340]
- [107] S. H. Hendi, S. Panahiyan and B. Eslam Panah, Prog. Theor. Exp. Phys. **103E01** (2015)
- [108] S. H. Hendi, B. Eslam Panah and S. Panahiyan, JHEP **11**, 157 (2015).
- [109] S. H. Hendi, B. Eslam Panah and S. Panahiyan, [arXiv:1510.00108].
- [110] F. Weinhold, J. Chem. Phys. **63**, 2479 (1975).
- [111] F. Weinhold, J. Chem. Phys. **63**, 2484 (1975).
- [112] H. Quevedo, J. Math. Phys. **48**, 013506 (2007);
- [113] H. Quevedo and A. Sanchez, JHEP **09**, 034 (2008);

- [114] H. Quevedo, *Gen. Relativ. Gravit.* **40**, 971 (2008).
- [115] S. H. Hendi, S. Panahiyan, B. Eslam Panah and M. Momennia, *Eur. Phys. J. C* **75**, 507 (2015).
- [116] S. H. Hendi, S. Panahiyan and B. Eslam Panah, *Adv. High Energy Phys.* **2015**, 743086 (2015).
- [117] S. H. Hendi, A. Sheykhi, S. Panahiyan and B. Eslam Panah, *Phys. Rev. D* **92**, 064028 (2015).
- [118] G. Ruppeiner, *Phys. Rev. A* **20**, 1608 (1979).
- [119] G. Ruppeiner, *Rev. Mod. Phys.* **67**, 605 (1995).
- [120] C. V. Johnson, *Class. Quantum Gravit.* **31**, 205002 (2014);
- [121] B. P. Dolan, *JHEP* **10**, 179 (2014).
- [122] E. Caceres, P. H. Nguyen and J. F. Pedrazab, *JHEP* **09**, 184 (2015).
- [123] B. P. Dolan, *Mod. Phys. Lett. A* **30**, 1540002 (2015).
- [124] S. H. Hendi, S. Panahiyan and R. Mamasani, *Gen. Relativ. Gravit.* **47**, 91 (2015).
- [125] J. Magueijo and L. Smolin, *Phys. Rev. D* **71**, 026010 (2005).
- [126] J. J. Peng and S. Q. Wu, *Gen. Relativ. Gravit.* **40**, 2619 (2008).
- [127] K. C. K. Chan, J. H. Horne and R. B. Mann, *Nucl. Phys. B* **447**, 441 (1995).
- [128] M. Ozer and M. O. Taha, *Phys. Rev. D* **45**, 997 (1992).
- [129] S. S. Yazadjiev, *Class. Quantum Gravit.* **22**, 3875 (2005).
- [130] A. Sheykhi and N. Riazi, *Phys. Rev. D* **75**, 024021 (2007).
- [131] M. H. Dehghani and N. Farhangkhah, *Phys. Rev. D* **71**, 044008 (2005).
- [132] L. F. Abbott and S. Deser, *Nucl. Phys. B* **195**, 76 (1982).
- [133] R. Olea, *JHEP* **06**, 023 (2005).
- [134] G. Kofinas and R. Olea, *Phys. Rev. D* **74**, 084035 (2006).
- [135] J. Magueijo and L. Smolin, *Phys. Rev. Lett.* **88**, 190403 (2002).
- [136] S. Gunasekaran, D. Kubiznak and R. B. Mann, *JHEP* **11**, 110 (2012).
- [137] S. H. Hendi and Z. Armanfard, *Gen. Relativ. Gravit.* **47**, 125 (2015).
- [138] M. H. Dehghani, S. Kamrani and A. Sheykhi, *Phys. Rev. D* **90**, 104020 (2014).
- [139] S. H. Hendi, S. Panahiyan, B. Eslam Panah, M. Momennia and M. S. Taleh Zadeh, *in preparation*.
- [140] S. H. Hendi, A. Dehghani and M. Faizal, *in preparation*.
- [141] S. H. Hendi and H. Behnamifard *in preparation*.

